

Synthesis and biological evaluation of phenylpropanoid derivatives

Sheng Liu^{1,2} · Yubin Li¹ · Wanxing Wei² · Jingchen Wei³

Received: 24 August 2015 / Accepted: 3 March 2016
© Springer Science+Business Media New York 2016

Abstract In this work, a series of oxime ether phenylpropanoid derivatives were synthesized. Their anti-hepatitis B virus (HBV) activity in HepG 2.2.15 cells was determined, and anti-cancer potential against three human cancer cell lines was evaluated. All the synthesized derivatives showed great efficiency against HBV. Compound 4d demonstrated the most effective anti-HBV activity, performing strong potent inhibitory not only on the secretion of HBsAg ($IC_{50} = 50.45 \mu M$, $SI = 9.18$) and HBeAg ($IC_{50} = 50.11 \mu M$, $SI = 9.24$), but also on the HBV DNA replication ($IC_{50} = 51.80 \mu M$, $SI = 8.94$). Besides, the synthetic compounds also displayed obvious anti-cancer activity. Moreover, the docking study of all synthesized compounds inside the related protein active site was conducted to explore the molecular interactions and a molecular target for activity using a MOE-docking technique. This study identified a new class of potent anti-HBV and anti-cancer agents.

Keywords Synthesis · Phenylpropanoid derivatives · Anti-HBV activity · Anti-cancer activity · Molecular docking

Introduction

Natural products and their derivatives possessing various skeletons could provide a great opportunity for novel drugs development (Gao *et al.*, 2011; Du *et al.*, 2011; Wang *et al.*, 2012). Lignans, one of the natural products, have been associated with several bioactivities ranging from anti-HBV, anti-HIV, anti-cancer, antioxidant and anti-inflammatory activities (Manat *et al.*, 2007; Saleem *et al.*, 2005; Yamashita *et al.*, 1992). Our previous study determined that lignans niranthin, nirtetralin, nirtetralin A and nirtetralin B isolated from *Phyllanthus niruri* L. exhibited significant anti-HBV activity (Wei *et al.*, 2012; Liu *et al.*, 2014a, b). Lignans hypophyllanthin, phyllanthin and a series of lignans isolated from *Cornus kousa* Burg. were found to possess anti-cancer and anti-inflammatory activity (Parvathaneni *et al.*, 2014). Globoidnan A from *Eucalyptus globoidea* and a series of lignans from *Kadsura interior* were reported as potent anti-HIV agents (Chen *et al.*, 1997; Ovenden *et al.*, 2004). These lignans are the most promising alternative to current novel drugs. However, only few of these complex products lignans exist in the nature. Hence, a method to synthesize these derivatives is necessary to approach their clinical function.

Hepatitis and cancer are two of the main life-threatening problems in the world, leading to millions of deaths every year (Lavanchy, 2004). Although various of drugs have been developed in HBV and cancer treatments, there is still a growing need for more effective agent with highly selectivity.

Lignans are composed of two molecular phenylpropanoid with the common C6-C3 structure. Lignans with anti-HBV and anti-cancer function are observed to possess some similar fragments in their molecular structure, including 3,4-dimethoxyphenyl, 3,4,5-trimethoxyphenyl,

✉ Sheng Liu
liusheng87@126.com

✉ Wanxing Wei
wxwei@gxu.edu.cn

¹ College of Science, Guangdong Ocean University, Zhanjiang 524088, People's Republic of China

² Department of Chemistry, Guangxi University, Nanning 530004, People's Republic of China

³ Department of Pharmacology, Guilin Medical University, Guilin 541004, People's Republic of China

benzo[d][1,3]dioxol-5-yl and 4-methoxybenzo[d][1,3]dioxol-5-yl. Therefore, in this work, (E)-3-(3,4-dimethoxyphenyl)acrylic acid (a), (E)-3-(3,4,5-trimethoxyphenyl)acrylic acid (b), (E)-3-(benzo[d][1,3]dioxol-5-yl)acrylic acid (c) and (E)-3-(7-methoxybenzo[d][1,3]dioxol-5-yl)acrylic acid (d) were chosen as the main scaffold for the design and synthesis of our anti-HBV and anti-cancer agents. Adamantyl substituent compounds were reported to possess special effects in clinical and used in flu virus, antitumor, artificial blood, treatment of Parkinson's disease and so on (Balzarini *et al.*, 2009). Thus, the acrylic acid and adamantane were considered to construct the scaffold in order to find stronger activity drugs. According to the molecular hybridization principle, esterification of natural compounds is a promising approach for derivatives synthesis, by which two active parts can be easily hybridized to enhance activity (Viegas-Junior, *et al.*, 2007; Chen *et al.*, 2014). Moreover, using oxime ester compounds obtained from the four acrylic acids and adamantane for anti-HBV and anti-cancer treatment were not reported before (Wu *et al.*, 2012; Kim *et al.*, 2000; Panda *et al.*, 2012a, b). Hence, in this work, a series of phenyl acryloyl type oxime esters based on the four acrylic acids were synthesized. The anti-HBV and anti-cancer activities of the compound were also evaluated in this work.

The study was further extended to prediction by a QSAR study to help know about the molecular properties (Santos *et al.*, 2009; Babu *et al.*, 2012). In addition, docking study was carried out to explore the molecular interactions and molecular targets for the activities of phenylpropanoid derivatives with the protein using molecular operating environment (MOE).

Materials and methods

General

Melting points were determined using electrothermal melting point apparatus WRX-4 (Shanghai, China) and were uncorrected. Mass spectroscopy was performed on a Finnigan LCQ Deca XP MAX mass spectrometer (Thermo Fisher, San Jose, CA, USA) which is equipped with an ESI source and an ion trap analyzer in the positive ion mode/in the negative ion. NMR spectra were recorded on Bruker AM 400 MHz ($^1\text{H}/^{13}\text{C}$, 400 MHz/100 MHz) or Bruker DRX 500 MHz ($^1\text{H}/^{13}\text{C}$, 500 MHz/125 MHz) spectrometer (Bruker, Bremerhaven, Germany) and chemical shifts were quoted in δ as parts per million (ppm) downfield with tetramethylsilane (TMS) as internal reference. Column chromatography (CC): silica gel (200–300 mesh; Qingdao Makall Group Co., Ltd., Qingdao, China). All reactions were monitored using thin layer chromatography (TLC) on

silica gel plates. Yields referred to isolated pure products and were not maximized. On the basis of NMR and HPLC (Thermo Fisher UItiMate 3000, USA) data, all final compounds reported in the manuscript were >95 % pure.

Chemistry (Scheme 1)

Preparation of 2-adamantanone oxime

Hydroxylamine hydrochloride (1.2 equiv, 12 mmol) and sodium acetate (1.2 equiv, 12 mmol) were added to a solution of the aldehyde (1 equiv, 10 mmol) in EtOH (50 mL). The reaction was stirred at 60 °C for 2 h. After the EtOH was removed by evaporating the solution in vacuo, the residue was suspended in DCM (50 mL) and washed with 1 M HCl solution (3×30 mL), H_2O (3×30 mL) and brine solution. The organic phase was dried (Na_2SO_4) and then concentrated at reduced pressure. The oximes 1–3 were purified by recrystallization.

2-adamantanone oxime Yield 100 %. m.p. 163–164 °C. ESIMS: m/z 166.4 $[\text{M} + \text{H}]^+$, calc. for $\text{C}_{10}\text{H}_{15}\text{NO}$ (165.23) (Terent'ev *et al.*, 2006).

Preparation for compounds 2a–2d

A mixture of compound 1 (1 equiv, 10 mmol), malonic acid (1.2 equiv, 12 mmol) and two drops of piperidine in pyridine (25 mL) was refluxed for 4 h and evaporated to remove pyridine. The residue was suspended in H_2O (30 mL) and extracted with EtOAc (2×50 mL) which was further purified by recrystallization to afford 2a–d.

(E)-3-(3,4-dimethoxyphenyl)acrylic acid (2a) Yield 82 %. m.p. 181–183 °C. ESIMS: m/z 208.0600 $[\text{M}]^+$, calc. for $\text{C}_{11}\text{H}_{12}\text{O}_4$ (208.21) (Brittelli *et al.*, 1981).

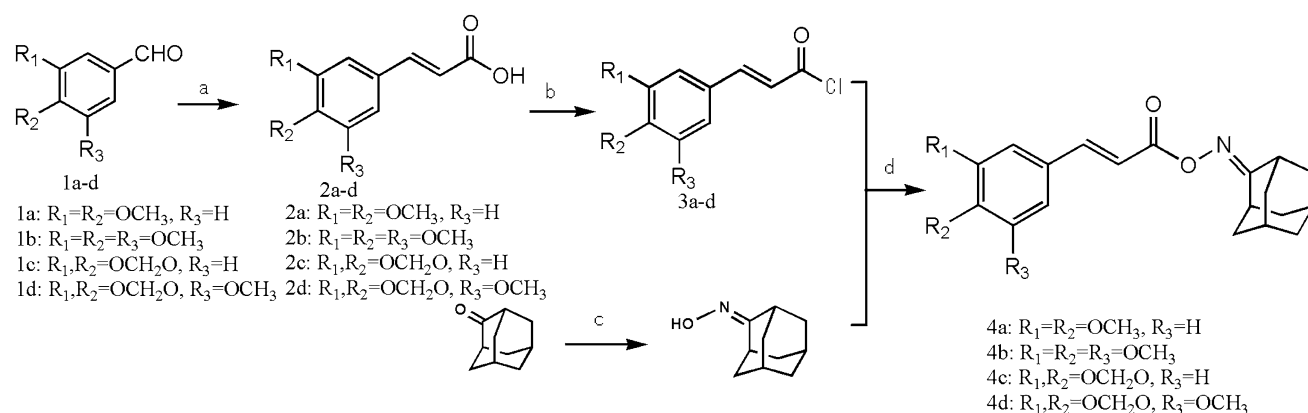
(E)-3-(3,4,5-trimethoxyphenyl)acrylic acid (2b) Yield 90 %. m.p. 126–127 °C. ESIMS: m/z 238.6 $[\text{M}]^+$, 237.6 $[\text{M}-\text{H}]^+$, calc. for $\text{C}_{12}\text{H}_{14}\text{O}_5$ (238.24) (Peterson *et al.*, 1988).

(E)-3-(benzo[d][1,3]dioxol-5-yl)acrylic acid (2c) Yield 85 %. m.p. 242–244 °C. ESIMS: m/z 192.2 $[\text{M}]^+$, 408.4 $[2\text{M} + \text{Na}]^+$, calc. for $\text{C}_{10}\text{H}_8\text{O}_4$ (192.17) (Salum *et al.*, 2010).

(E)-3-(7-methoxybenzo[d][1,3]dioxol-5-yl)acrylic acid (2d) Yield 80 %. m.p. 228–229 °C. ESIMS: m/z 221 $[\text{M}-\text{H}]^+$, calc. for $\text{C}_{11}\text{H}_{10}\text{O}_5$ (222.19) (Salway, 1909).

Preparation for cinnamoyl chlorides 3a–3d

Substituted cinnamoyl chlorides were obtained by refluxing the appropriate acid 2a–d (10 mmol) with thionyl chloride (10 mL) for 5 h. After evaporation at reduced pressure, the



Scheme 1 Synthetic route to the series of compounds. Reagents and conditions: *a* $\text{CH}_2(\text{COOH})_2$, piperidine, $\text{C}_5\text{H}_5\text{N}$, reflux, 4 h, 80–90 %; *b* SOCl_2 , CH_2Cl_2 , reflux, 5 h, 95 %; *c* $\text{H}_2\text{NOH-HCl}$, AcONa , EtOH , 60 °C, 1 h, 98 %; *d* Et_3N , CH_2Cl_2 , rt, 12 h, 50–70 %

crude liquid residue was used for subsequent reactions without purification.

Preparation for compounds 4a–4d

Oxime (1 equiv, 10 mmol) was resolved in dry DCM (20 mL), then triethylamine (TEA) (1.2 equiv, 12 mmol) was added drop wise to the solution at 0 °C, and then reaction mixture was stirred for 30 min at 0 °C. Appropriate acid chloride (1 equiv, 10 mmol) was added to the mixture, and then reaction mixture was stirred for 10–20 min at 0 °C, for 12 h at room temperature. DCM was evaporated to dryness. The residue was washed with cold ether (5 mL) and hot water and then purified by column chromatography on silica gel eluting with ethyl acetate/petroleum ether 1:1–3:1.

(E)-2-adamantanone-2-carbaldehyde O-3-(3,4-dimethoxyphenyl)acryloyl oxime (4a) White crystal, yield 67 %. m.p. 127.6–127.8 °C. ^1H NMR (400 MHz, CDCl_3): δ 1.86–2.00 (14H, m, H-adamantane), 3.89 (6H, each 3H, s, H-20, 21), 6.36 (1H, d, $J = 15.91$, H-8), 6.85 (1H, d, $J = 8.28$, H-5), 7.05 (1H, d, $J = 1.79$, H-2), 7.11 (1H, dd, $J = 1.79, 8.28$, H-6), 7.71 (1H, d, $J = 15.91$, H-7). ^{13}C NMR (100 MHz, CDCl_3): δ 174.80 (C-9), 165.52 (C-10), 151.19 (C-3), 149.14 (C-4), 145.38 (C-7), 127.35 (C-1), 122.81 (C-6), 113.76 (C-8), 110.97 (C-5), 109.53 (C-2), 55.96, 55.86 (C-20, 21), 38.85, 37.77, 36.17 (C-12, 14, 16, 17, 19), 36.14, 31.21, 27.48 (C-11, 13, 15, 18). ESIMS: m/z 356.188 $[\text{M} + \text{H}]^+$, 378.344 $[\text{M} + \text{Na}]^+$, 735.488 $[2\text{M} + \text{H} + \text{Na}]^+$, calc. for $\text{C}_{21}\text{H}_{25}\text{NO}_4$ (355.43).

(E)-2-adamantanone-2-carbaldehyde O-3-(3,4,5-trimethoxyphenyl)acryloyl oxime (4b) White crystal, yield 69 %. m.p. 158.6–158.9 °C. ^1H NMR (500 MHz, CDCl_3): δ 1.87–2.07 (14H, m, H-adamantane), 3.89 (9H, each 3H, s, H-20, 21, 22), 6.42 (1H, d, $J = 15.92$, H-8), 6.79 (2H, s, H-2, 6), 7.71 (1H, d, $J = 15.92$, H-7). ^{13}C NMR

(125 MHz, CDCl_3): δ 174.96 (C-9), 165.23 (C-10), 153.41 (C-3, 5), 145.42 (C-7), 140.21 (C-4), 129.88 (C-1), 115.41 (C-8), 105.30 (C-2, 6), 60.95 (C-21), 56.15 (C-20, 22), 38.87, 37.80, 36.18 (C-12, 14, 16, 17, 19), 36.16, 31.24, 27.49 (C-11, 13, 15, 18). DEPT135: δ 174.96, 165.23, 153.41, 140.21, 129.88 (C), 145.42, 115.41, 105.30, 36.16, 31.24, 27.49 (CH), 38.87, 37.80, 36.18 (CH_2), 60.95, 56.15 (CH_3). ESIMS: m/z 386.3 $[\text{M} + \text{H}]^+$, 408.2 $[\text{M} + \text{Na}]^+$, calc. for $\text{C}_{22}\text{H}_{27}\text{NO}_5$ (385.45).

(E)-2-adamantanone-2-carbaldehyde O-3-(benzo[d][1,3]-dioxol-5-yl)acryloyl oxime (4c) White crystal, yield 66 %. m.p. 119.6–120.0 °C. ^1H NMR δ 1.82–1.99 (14H, m, H-adamantane), 6.05 (2H, s, H-20), 6.44 (1H, d, $J = 15.90$, H-8), 6.85 (1H, d, $J = 7.95$, H-5), 6.95 (1H, s, H-2), 6.98 (1H, d, $J = 7.95$, H-6), 7.77 (1H, d, $J = 15.90$, H-7). ^{13}C NMR (100 MHz, CDCl_3): δ 174.76 (C-9), 166.80 (C-10), 150.80 (C-3), 148.84 (C-4), 145.40 (C-7), 127.31 (C-1), 121.67 (C-6), 113.84 (C-8), 109.93 (C-5), 106.95 (C-2), 101.85 (C-20), 38.88, 37.48, 36.51 (C-12, 14, 16, 17, 19), 36.23, 28.78, 27.86 (C-11, 13, 15, 18). DEPT135: δ 174.76, 166.80, 150.80, 148.84, 127.31 (C), 145.40, 121.67, 113.84, 109.93, 106.95, 36.23, 28.78, 27.86 (CH), 101.85, 38.88, 37.48, 36.51 (CH_2). ESIMS: m/z 678.3 $[2\text{M}]^+$, 679.0 $[2\text{M} + \text{H}]^+$, 701.1 $[2\text{M} + \text{Na}]^+$, calc. for $\text{C}_{20}\text{H}_{21}\text{NO}_4$ (339).

(E)-2-adamantanone-2-carbaldehyde O-3-(7-methoxybenzo[d][1,3]-dioxol-5-yl)acryloyl oxime (4d) White crystal, yield 65 %. m.p. 159.1–159.5 °C. ^1H NMR (500 MHz, CDCl_3): δ 1.89–2.06 (14H, m, H-adamantane), 3.93 (3H, s, H-21), 6.02 (2H, s, H-20), 6.35 (1H, d, $J = 15.84$, H-8), 6.73 (1H, d, $J = 1.36$, H-6), 6.78 (1H, d, $J = 1.36$, H-2), 7.67 (1H, d, $J = 15.84$, H-7). ^{13}C NMR (125 MHz, CDCl_3): δ 174.94 (C-9), 165.38 (C-10), 149.38 (C-5), 145.23 (C-7), 143.71 (C-3), 137.49 (C-4), 129.26 (C-1), 114.68 (C-8), 109.35 (C-6), 102.03 (C-20), 101.33 (C-2), 56.63 (C-21), 38.90, 37.81, 36.22 (C-12, 14, 16, 17, 19), 36.18, 31.26, 27.53 (C-11, 13, 15, 18).

Table 1 Anti-HBV activity and cytotoxicity of the phenylpropanoid derivatives in vitro^a

Compound	CC ₅₀ ^b (μM)	HBsAg ^c		HBeAg ^d		HBV DNA replication	
		IC ₅₀ ^e (μM)	SI ^f	IC ₅₀ ^e (μM)	SI ^f	IC ₅₀ ^e (μM)	SI ^f
2-adamantanone	635.25	—	—	—	—	—	—
Oxime	475.21	479.80	1.01	519.47	0.91	—	—
1a	>1500	— ^g	—	—	—	—	—
1b	>1500	—	—	—	—	—	—
1c	1289.31	—	—	—	—	—	—
1d	1075.75	—	—	—	—	—	—
2a	534.66	>600	<0.89	>600	<0.89	—	—
2b	834.13	>600	<1.39	>600	<1.39	—	—
2c	503.46	433.15	1.16	526.25	0.96	—	—
2d	667.25	410.96	1.62	476.75	1.40	—	—
4a	385.46	120.46	3.20	125.50	3.07	—	—
4b	506.99	107.19	4.73	74.80	6.78	141.46	3.58
4c	358.48	67.17	5.34	71.97	4.98	97.36	3.68
4d	463.07	50.45	9.18	50.11	9.24	51.80	8.94
3TC ^h	568.25	152.00	3.74	181.72	3.13	6.86	82.84

^a Values are means determined from at least two experiments^b CC₅₀ is 50 % cytotoxicity concentration in HepG2 2.2.15 cells^c HBsAg: hepatitis B surface antigen^d HBeAg, hepatitis B e antigen^e IC₅₀ is 50 % inhibitory concentration^f SI (selectivity index) = CC₅₀/IC₅₀^g No SI can be obtained^h Lamivudine (3TC) as the positive control

DEPT135: δ 174.94, 165.38, 149.38, 143.71, 137.49, 129.26 (C), 145.23, 114.68, 109.35, 101.33, 36.18, 31.26, 27.53 (CH), 102.03, 38.90, 37.81, 36.22 (CH₂), 56.63 (CH₃). ESIMS: m/z 370.1662 [M + H]⁺, 392.1489 [M + Na]⁺, calc. for C₂₁H₂₃NO₅ (369.41).

Pharmacology

Anti-HBV potential determination

The anti-HBV activity of the compound was tested as previously described (Liu *et al.*, 2015). Briefly, the HepG2.2.15 cells, provided by the Chinese Academy of Medical Sciences (P.R. China), were selected as the tumor cell model. 200 μL of the HepG2.2.15 suspension (Density: 1×10^5 cells/mL) was placed in each aperture of a 96-well microtiter plates under 5 % CO₂ at 37 °C. The HepG2.215 was incubated for 24 h before the addition of drug sample at various concentrations. Lamivudine (3TC) was served as the positive control. Cells were referred with drug-containing fresh medium every 3 days for up to 9 days in time-

dependent experiment. Medium was taken at third day of treatment (T_3), the sixth day of treatment (T_6) and the ninth day of treatment (T_9), and stored at −20 °C before analysis. The IC₅₀ and the selected index (SI) of each compound were calculated, respectively. After drug treatment, the cytotoxicity of the drugs was measured using the MTT assay (Ferrari *et al.*, 1990; Han *et al.*, 2008).

The levels of HBV surface antigen (HBsAg) and HBV e antigen (HBeAg) were simultaneously detected using ELISA kits (Rongsheng Biotechnology Co. Ltd, Shanghai, China) according to the manufacturer's instructions.

Inhibitory activity against HBV was determined using a real-time fluorescence quantitative PCR (FQ-PCR). The determination process was described in our previous work (Liu *et al.*, 2014a, b). Briefly, 2.0 μL of HBV DNA was amplified in a 25 mL of mixture which contained 12.5 μL 2 × SYBR Green Master (ROX) and 2 primers. These two primers are specifically designed for HBV, including a forward primer (5'-AAC CAT TGA AGC AAT CAC TAG AC-3') and a reverse primer (5'-ATC TAT GGT GGC TGC TCG AAC TA-3'). The thermal program was comprised with an initial denaturation at 95 °C for 10 min

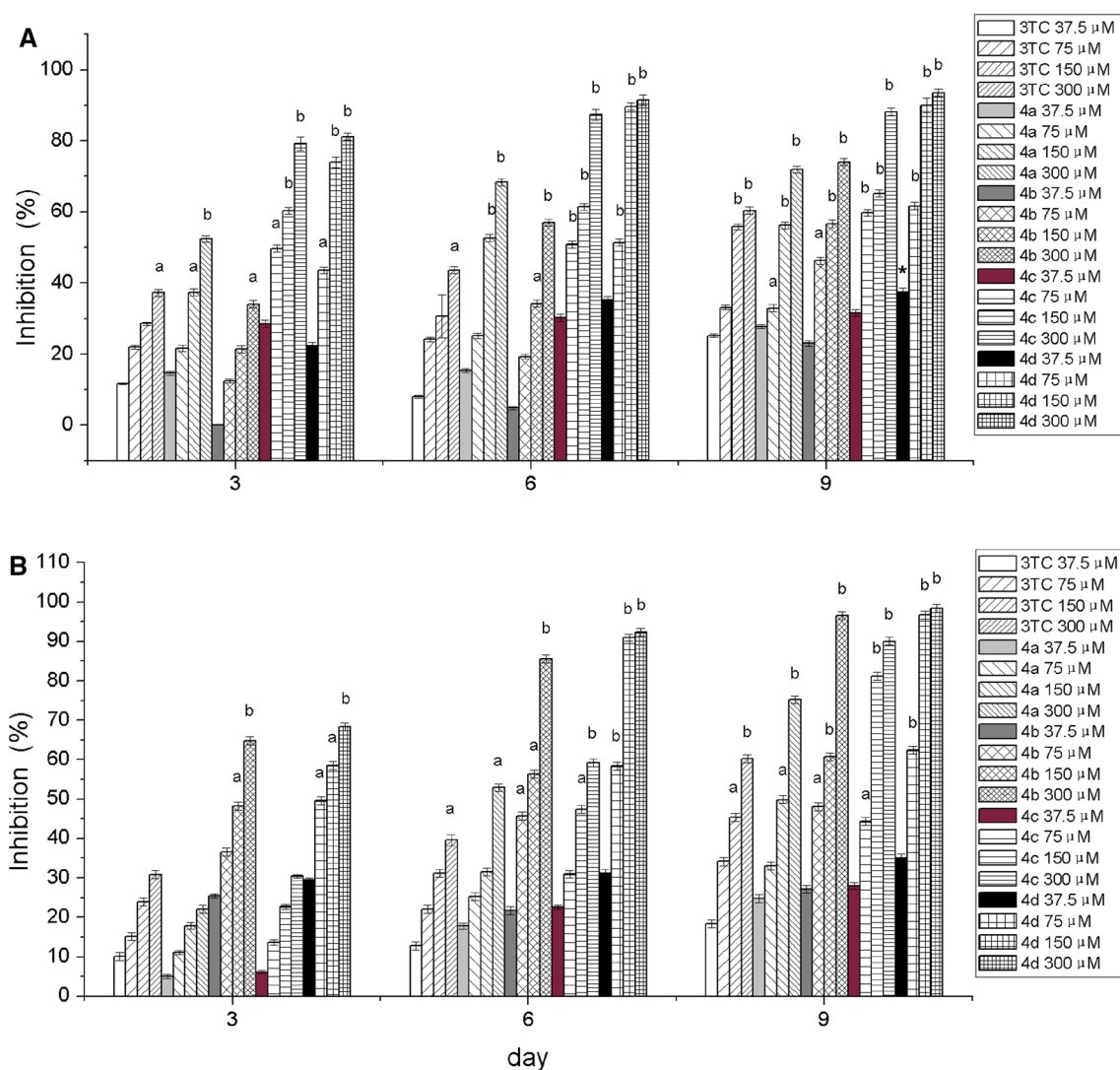


Fig. 1 Inhibitory effect of the phenylpropanoid derivatives on secretion of HBsAg (a) and HBeAg (b) in the HepG2.2.15 cell line. Data were expressed as mean \pm SE ($n = 3$). ^a $P < 0.05$, ^b $P < 0.01$ compared to control

followed by 40 amplification cycles with each of the two following steps: 95 °C for 15 s and 60 °C for 1 min.

Anti-cancer potential determination

Anti-cancer activities of the compounds were identified using the MTT assay on lung cancer cell line A549, hepatic cancer cell line SMMC-7721 and gastric cancer cell line SMMG-803. Logarithmically growing cells were seeded in 96-well culture plates at a density of 1×10^5 cells/mL in 5 % CO₂ at 37 °C. After 24-h incubation, various concentrations of drugs at different concentrations were added into the cell sample. The mixture suspension was then incubated for another 48 h. The synthesized compounds, with cis-platinum as positive control, were evaluated in duplicate at

final concentrations ranging from 0.0945 to 1.5 mM. After the incubation, the culture media was removed, 180 μ L fresh media and 20 μ L of MTT solution (5 mg/mL) were added into each well. The suspension was then incubated for another 4 h. After the incubation, the culture media was removed again. After the addition of 100 μ L of DMSO, the OD values were measured using a microplate reader at 490 nm and the percent of cell death was calculated.

Molecular docking simulation

Ligand study was performed with HyperChem software. The 3D structures of the synthesized compounds were constructed and optimized, and then QSAR descriptors were studied, which is a powerful lead optimization tool

Table 2 Anti-cancer activity of the phenylpropanoid derivatives in vitro

Compound	Concentration/mM	A549		SMMC-7721		SMMG-803	
		Inhibition/%	IC ₅₀ /mM	Inhibition/%	IC ₅₀ /mM	Inhibition/%	IC ₅₀ /mM
4a	0.094	86.27	—	82.47	—	84.88	—
	0.188	87.00		84.27		84.97	
	0.375	87.92		85.24		85.53	
	0.75	88.91		85.47		85.72	
	1.5	88.93		85.98		85.77	
4b	0.094	22.54	0.443	83.72	—	35.88	0.225
	0.188	32.96		85.06		44.24	
	0.375	51.20		85.15		55.30	
	0.75	58.57		85.61		74.71	
	1.5	71.34		86.16		84.37	
4c	0.094	31.98	0.275	83.16	—	59.45	—
	0.188	37.13		84.59		76.53	
	0.375	60.11		84.59		83.25	
	0.75	69.76		85.10		83.62	
	1.5	77.79		86.07		85.39	
4d	0.094	5.92	0.513	16.74	0.276	1.40	0.407
	0.188	9.97		18.93		12.13	
	0.375	29.83		84.46		84.27	
	0.75	72.52		86.39		86.33	
	1.5	88.08		85.82		85.72	
Cis-platinum	0.094	65.71	—	83.76	—	67.90	—
	0.188	70.04		83.90		83.11	
	0.375	70.53		84.29		84.97	
	0.75	72.56		85.26		85.16	
	1.5	74.83		85.29		85.49	

Table 3 Molecular descriptors of derivatives from QSAR study

Ligand	Molecular weight (Da)	LogP	Molar refractivity (Å ³)	Surface area (Å ²)	Volume (Å ³)	Hydration energy (Kcal/mol)	Polarizability (Å ³)
3TC	229.25	−0.55	55.14	525.55	606.87	48.20	21.71
2a	208.21	−0.6	59.95	306.89	324.12	55.67	21.41
2b	238.24	−1.59	66.32	348.16	346.69	56.46	23.89
2c	192.17	−0.14	52.79	303.06	302.58	53.96	18.80
2d	222.19	−1.40	59.16	348.41	330.85	54.82	21.28
4a	355.43	2.32	103.17	555.34	1036.38	60.65	38.38
4b	385.45	1.32	109.54	609.17	1098.41	60.41	40.85
4c	339.39	2.51	96.01	566.06	961.22	58.30	35.77
4d	369.41	1.51	102.38	612.68	1030.68	57.18	38.24

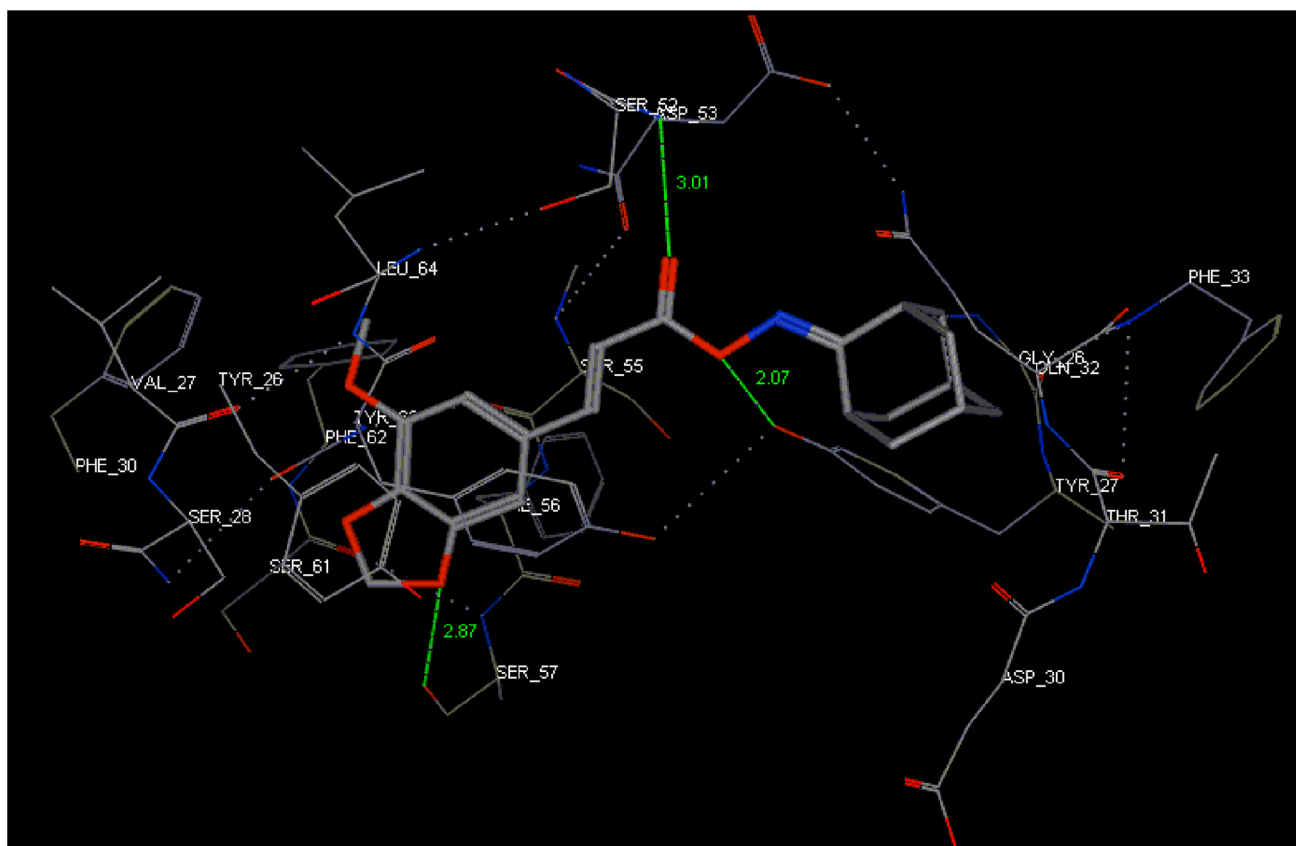
that can quantitatively relate variations in biological activity to changes in molecular properties.

Molecular docking study was performed using MOE 2008.10 to illuminate the ligand–protein interactions in detail.

The target compounds were built using the builder interface of the MOE program and subjected to energy minimization. The crystal structure of protein was retrieved from Protein Data Bank (<http://www.rcsb.org/pdb/home/home.do>) (Liu

Table 4 Docking score and binding into 3OX8

Ligand	S-score (kcal/mol)	No. of H-bonds	Distance (Å)	Amino acid involved	Molecular structure
3TC	−10.7074	2	2.03	TYR 27	O of −OH
			2.29	TYR 27	O of −COC−
4a	−13.2226	3	2.94	SER 57	O of 3 −OCH ₃
			3.03	ASP 53	O of −C=O
			1.94	TYR 27	O of −ON
			3.01	SER 57	O of 3 −OCH ₃
4b	−15.6072	3	2.92	ASP 53	O of −C=O
			2.05	TYR 27	O of −ON
			2.80	SER 57	O of 3 −OCH ₃
			3.09	ASP 53	O of −C=O
4c	−15.6424	3	1.98	TYR 27	O of −ON
			2.87	SER 57	O of 3 −OCH ₃
			3.01	ASP 53	O of −C=O
4d	−16.9302	3	2.07	TYR 27	O of −ON

**Fig. 2** Binding mode of 4d into the binding site of HLA-A. The hydrogen bond formed colored in *green* (Color figure online)

et al., 2011). HBV-related protein Human leukocyte antigen (HLA-A) (PDB ID: 3OX8) was used to study the interactions between ligand and HBV protein in the active site. Lung cancer-related protein 3WDZ, hepatic cancer-related protein 3QBY and gastric cancer-related protein 4OUM were used

for anti-cancer study. The edited crystal structure after removing water molecules was imported into MOE. Chain A was considered for docking process as the protein is a dimer consisting of A and B chains. The structure was protonated, and polar hydrogens were added. And energy minimization

was performed till the gradient convergence 0.05 kcal/mol that reached to get the stabilized conformation. The active site was correlated with 'Site Finder' module of MOE to define the docking site for the ligands. Docking procedure was followed the standard protocol implemented in MOE 2008.10, and the geometry of resulting complexes was studied using the MOE's Pose Viewer.

Results and discussion

Chemistry

General synthesis for the intermediate and target compounds is depicted in Scheme 1. 2-Adamantanone was reacted with hydroxylamine hydrochloride in EtOH in the presence of sodium acetate to yield 2-adamantanone oxime in a good yield (Quan *et al.*, 2013). Intermediates 2a–d were prepared by Knoevenagel condensation of malonic acid and the aldehyde group of four benzaldehydes with yields of 80–90 % (Zou *et al.*, 2010). The final oxime ester derivatives 4a–4d were obtained by reaction of oxime with cinnamoyl chloride 3a–d in the presence of TEA, which was obtained by reaction of

substituted phenylacrylic acid 2a–d and thionyl chloride in DCM (Karakurt *et al.*, 2012).

The structures of the newly synthesized compounds 4a–4d were characterized by ^1H NMR, ^{13}C NMR and MS. Corresponding data are presented in the experimental Sect. ^1H NMR spectra of the derivatives showed two doublets at 6.35–6.44 and 7.67–7.77 ppm with $J = 15.84$ – 15.92 Hz corresponding to trans hydrogens of $\text{CH}=\text{CH}$, respectively. The singlet at 3.89–3.93 ppm attributed to $\text{O}-\text{CH}_3$ protons, and at 6.02–6.05 corresponded to OCH_2O protons. The chemical shifts of aromatic hydrogens of the phenyl ring appeared as multiplets in the region δ 6.73–7.11. ^{13}C NMR chemical shifts for title compounds were observed in their expected regions. ^{13}C NMR spectrum for the derivatives showed signals at 55.86–60.95, 101.85–102.03, 165.23–166.80 and 174.76–174.96 corresponding to CH_3 , CH_2 , $\text{C}=\text{N}$ and $\text{C}=\text{O}$, respectively.

Biological evaluation

Anti-HBV activity

All the newly synthesized derivatives were tested for their anti-HBV activity, namely inhibiting the secretion of

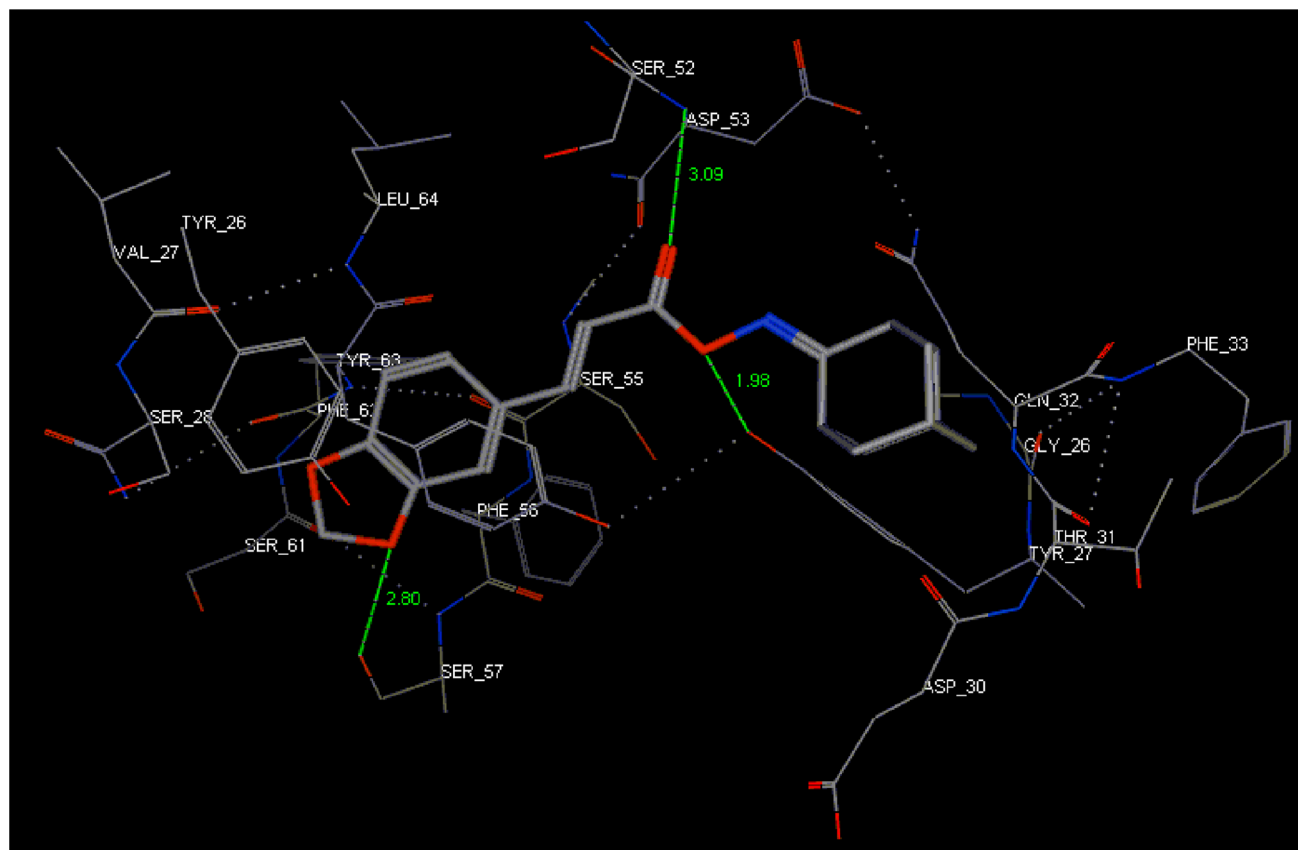


Fig. 3 Binding mode of 4c into the binding site of HLA-A. The hydrogen bond formed colored in green (Color figure online)

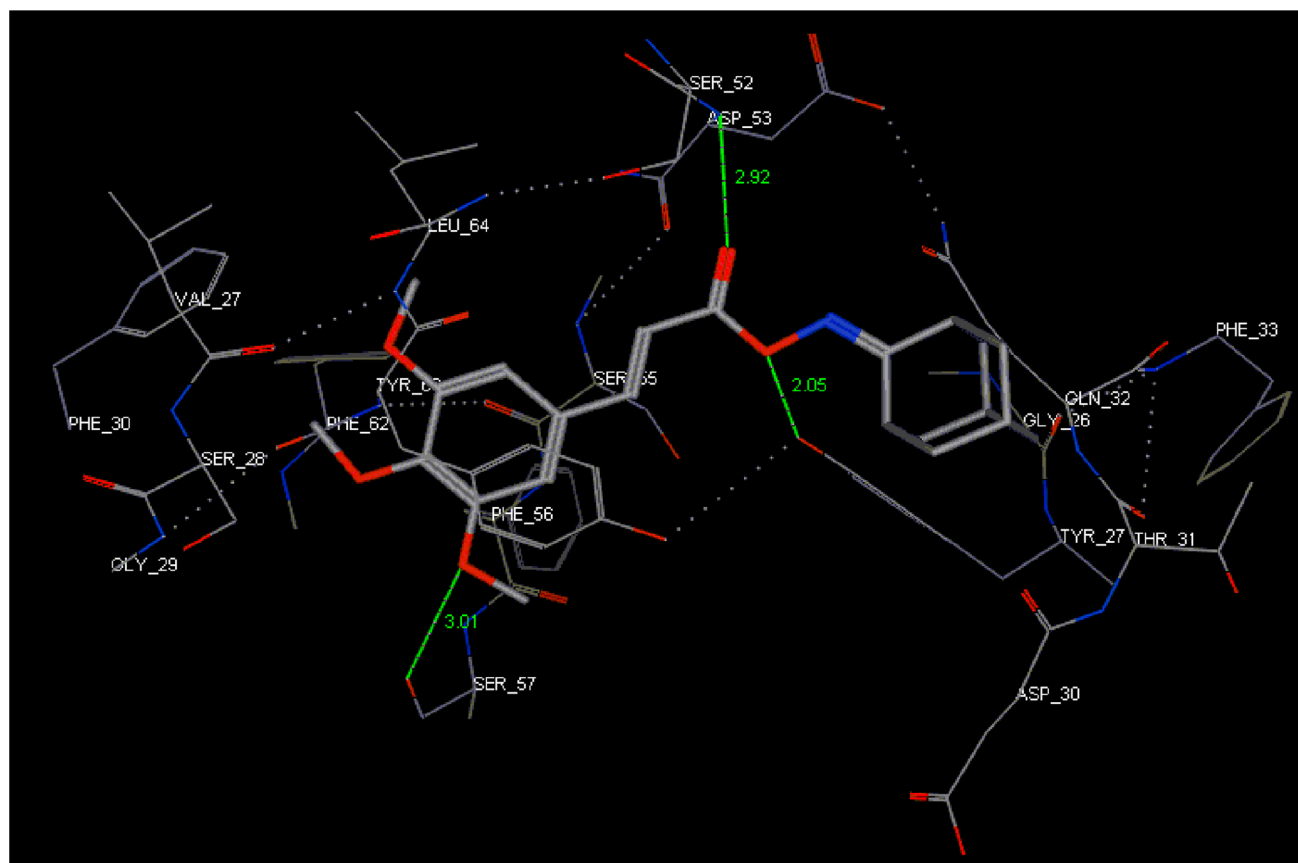


Fig. 4 Binding mode of 4b into the binding site of HLA-A. The hydrogen bond formed colored in *green* (Color figure online)

HBsAg, and HBeAg in HepG 2.2.15 cells. Positive control was conducted using lamivudine (3TC, a clinically popular anti-HBV agent) against the same HBV samples. The anti-HBV activity of each compound was evaluated using their IC₅₀ concentration against the secretion of HBsAg and HBeAg. And the cytotoxicity of each compound was determined by their concentration at which they could inhibit 50 % (CC₅₀) of the HepG 2.2.15 cells. Ratios between CC₅₀ and IC₅₀ of each compound was calculated to obtain their selectivity index (SI). The results of their anti-HBV activity and cytotoxicity are summarized in Table 1. The start reactants substituted benzaldehyde 1a–d, 2-adamantanone, intermediates 2a–d and oximes 1–3 showed low suppressant properties on the HBV while most of the derivatives showed high potency activity against the secretion of HBsAg and HBeAg as shown in Table 1.

The treatment of HBV-transfected HepG2.2.15 cells with various concentrations of drugs for 9 d exhibited a time- and dose-dependent inhibitory effect on the secretion of HBsAg and HBeAg (Fig. 1). All the derivatives were observed to show higher inhibitory activity against the secretion of HBsAg and HBeAg than lamivudine. Compound 4d showed the most potent anti-HBV activity, demonstrating potent inhibitory effect on the secretion of

HBsAg (IC₅₀ = 50.45 μM, SI = 9.18) and HBeAg (IC₅₀ = 50.11 μM, SI = 9.24).

Importantly, the inhibition of these compounds on HBV DNA replication was also investigated using lamivudine as the reference drug. Compounds 4b, 4c, and 4d exhibited anti-HBV activity with their IC₅₀ values against HBV DNA replication of 141.46, 97.36, 51.80 μM, respectively. Compounds 4b, 4c, and 4d displayed inhibiting not only HBsAg and HBeAg secretion but also HBV DNA replication. 3TC showed more significant activity against HBV DNA replication (IC₅₀ = 6.86), while it showed little inhibitory on HBsAg and HBeAg secretion.

Anti-cancer activity

The in vitro anti-cancer activities of the synthesized compounds against three human cancer cell lines (lung cancer cell line A549, hepatic cancer cell line SMMC-7721 and gastric cancer cell line SMMG-803) were evaluated using an MTT assay with cis-platinum as positive control. The results are shown in Table 2.

Compounds 4a displayed the most potent anti-cancer activity against cell lines A549, SMMC-7721, SMMG-803

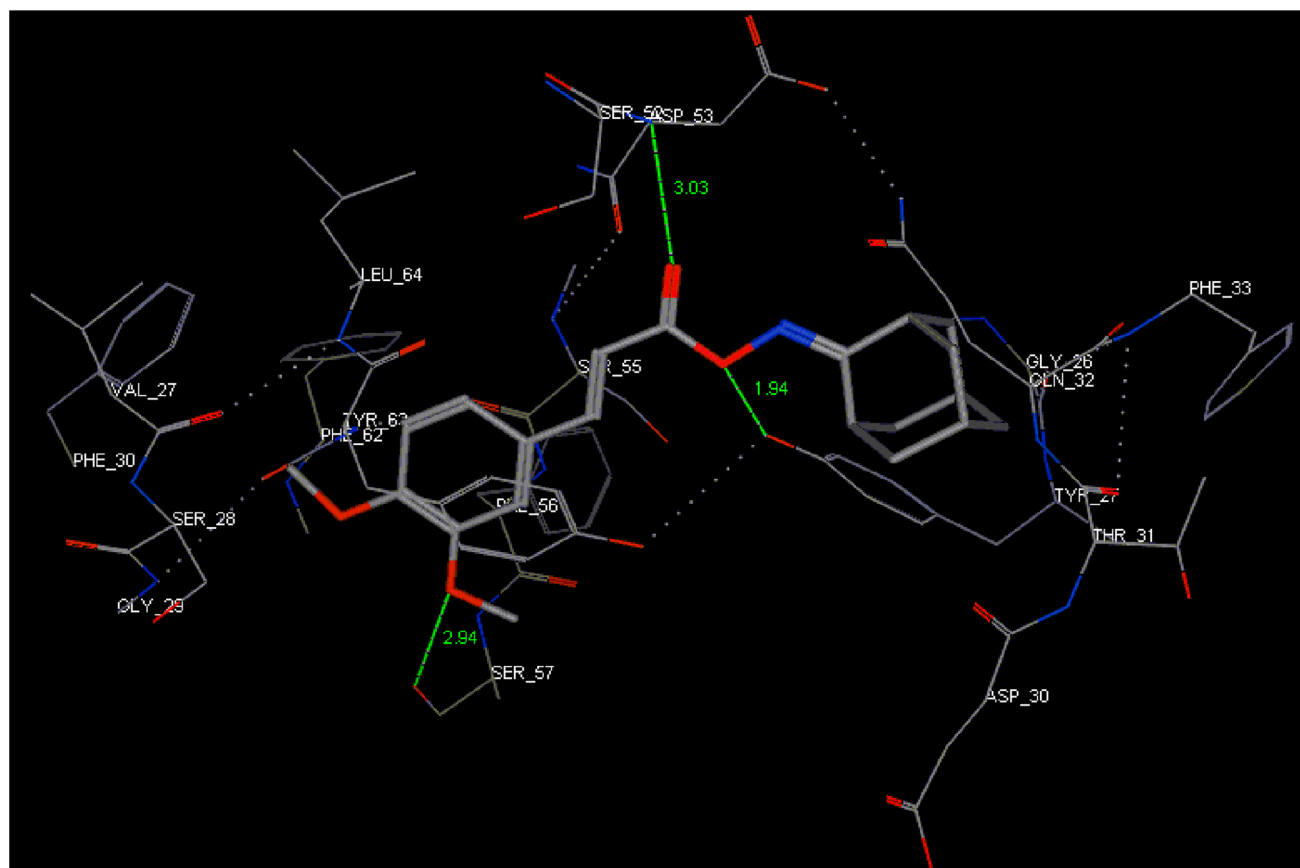


Fig. 5 Binding mode of 4a into the binding site of HLA-A. The hydrogen bond formed colored in *green* (Color figure online)

Table 5 Docking score and binding into 3WDZ, 3QBY and 4OUM

Ligand	S-score (kcal/mol)		
	3WDZ	3QBY	4OUM
4a	−15.3414	−15.8125	−14.6212
4b	−15.5431	−15.9114	−15.1279
4c	−16.1699	−14.3159	−14.4864
4d	−16.9997	−15.6494	−15.0533

with a mean growth inhibitions of 88.93, 85.98 and 85.77 %, respectively. The inhibition was higher than that of the positive control. The half maximal (50 %) inhibitory concentration (IC_{50}) of these compounds was measured as well. Compounds 4d exhibited anti-cancer activity with their IC_{50} values against A549, SMMC-7721 and SMMG-803 of 0.513, 0.276, 0.407 mM, respectively.

QSAR study

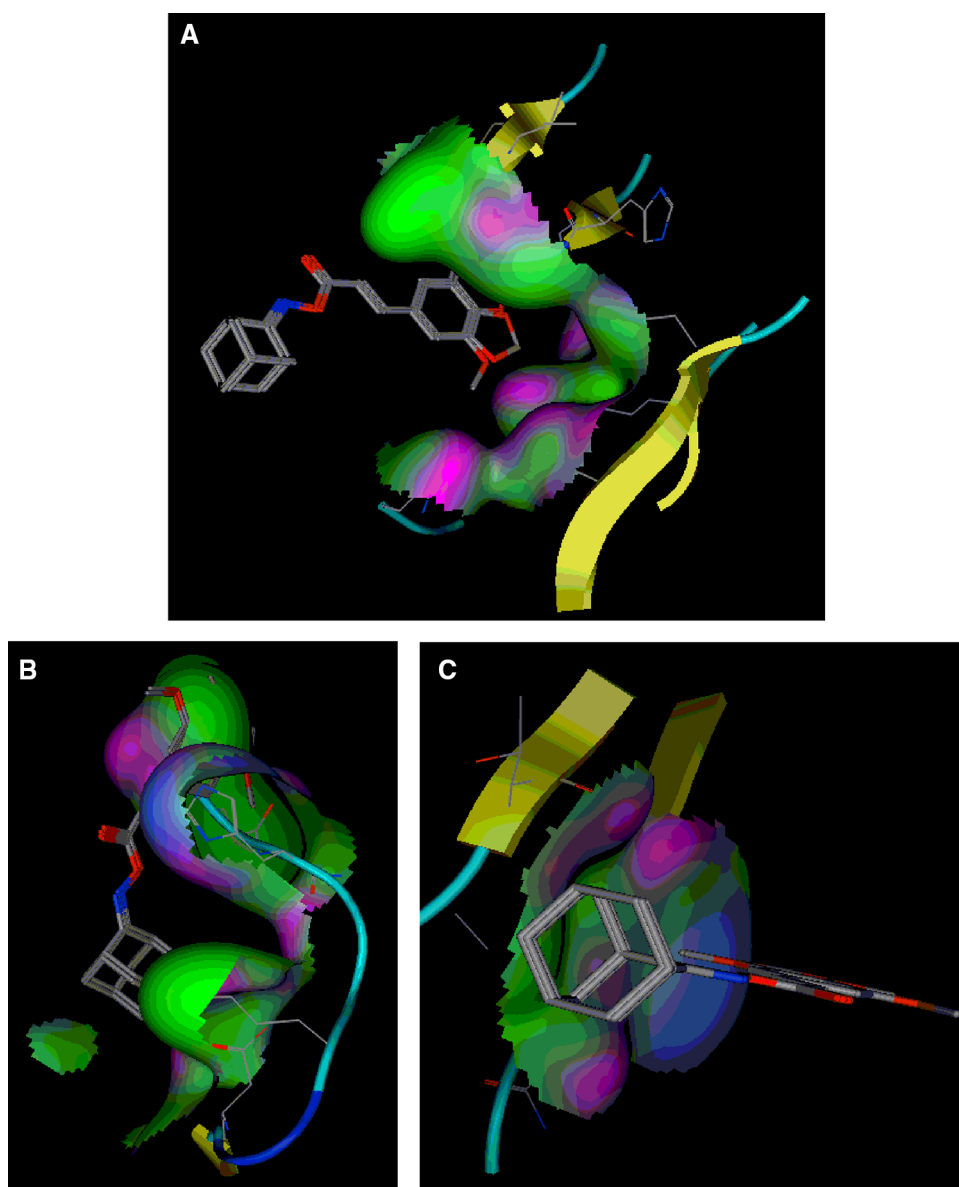
The 3D structures of all the compounds were generated using Built Optimum option of Hyperchem (version 8.0). Subsequently energy was minimized using MM + force field. The structures of all the compounds were fully

optimized. Molecular descriptors were determined by QSAR study, including $\log P$, molar refractivity, surface area, volume, hydration energy and polarizability, and the results showing that all molecules have drug like properties (Table 3). All the compounds have the molecular weight in the range from 190 to 390 Da. The $\log P$ values of these compounds laid in the region between 1.59 and 2.51, indicating their superior to act as drug. Their molar refractivity is in the range of 50–110.

Molecular docking

Molecular docking studies of phenylpropanoid derivatives were carried out using MOE 2008.10 as the docking

Fig. 6 Compounds Binding into the active pockets of 3WDZ (a), 3QBY (b) and 4OUM (c)



software in order to rationalize the biological activity results and understand the various interactions between ligand and protein in the active site in detail. The crystal structure of HLA-A protein (PDB ID: 3OX8), which is associated with severe liver inflammation in Chinese patients with chronic HBV infection, was used for anti-HBV study. Lung cancer-related protein 3WDZ, hepatic cancer-related protein 3QBY and gastric cancer-related protein 4OUM were used to identify the anti-cancer activity of our compounds. The ‘Site Finder’ tool of the program was used to search for its active site. We performed three docking procedures for each ligand and the best configuration of each of the ligand-receptor complexes was selected based on energetic grounds. The affinity

scoring function δG was used to assess and rank the receptor–ligand complexes.

The synthesized series derivatives had dock score with 3OX8 ranging from -13.2226 to -16.9302 (Table 4). Compound 4d was showing the best least docking score of -16.9302 , and the next best least docking score was found with 4c followed by 4b. Compound 4d was found to be forming three hydrogen bonds of lengths 2.87, 3.01 and 2.07 Å each with 3-OCH₃ in benzene ring of Ser57, carbonyl (C=O) of Asp53 and O–N in oxime ester group of Tyr27, respectively (Fig. 2). Compound 4c also formed three hydrogen bonds of lengths 2.80, 3.09 and 1.98 Å with 3-OCH₃ in benzene ring of Ser57, carbonyl (C=O) of Asp53 and O–N in oxime ester group of Tyr27 (Fig. 3).

Docking study of compound 4b and 4a with HLA-A receptor is shown in Figs. 4 and 5, respectively. In the docking study, we also found that the O of O–N in the oxime ester group interacted with Tyr27 by hydrogen bond.

In order to predict the possible binding mode of the compounds of the three kinds of cancers, compounds were docked into the related protein 3WDZ, 3QBY and 4OUM binding site of related cancer. The docking results are shown in Table 5. As shown in Fig. 6, compounds were completely binded into the active pockets of 3WDZ, 3QBY and 4OUM. The compounds interacted with 3WDZ through Van der waals interaction with residue ArgA380, GlyA433, CysA434 and GlnB356. Then, they interacted with 3QBY by interaction with residue MetA1, LysA6, AspA9 and HisA3.

Conclusion

In summary, our design and synthesis have led to four oxime ether phenylpropanoid derivatives by attaching of 2-adamantanone oxime to cinnamic acids. Then we screened their anti-HBV activity in HepG 2.2.15 cells and anti-cancer activities against three human cancer cell lines. All the derivatives displayed potent anti-HBV activity with the SI_{HBsAg} values from 3.20 to 9.18 and SI_{HBeAg} values from 3.07 to 9.24, in which compound 4d showed the most potent anti-HBV activity, demonstrating potent inhibitory effect not only on the secretion of HBsAg (IC_{50} = 50.45 μ M, SI = 9.18) and HBeAg (IC_{50} = 50.11 μ M, SI = 9.24) but also on HBV DNA replication (IC_{50} = 51.80 μ M, SI = 8.94). Then the synthetic compounds also exhibited potent anti-cancer activity. In addition, the docking study of all synthesized compounds inside the related protein active site was carried out to explore the molecular interactions and a molecular target for the activity using a MOE-docking technique. This study identified a new class of potent anti-HBV and anti-cancer agents.

Acknowledgments This work was financially supported by the national natural science foundation of China, natural science foundation of Guangxi province, China, and science research and technology development foundation of Guangxi province, China.

References

- Babu KR, Rao VK, Kumar YN, Polireddy K, Subbaiah KV, Bhaskar M, Lokanatha V, Raju CN (2012) Identification of substituted [3, 2-a] pyrimidines as selective antiviral agents: molecular modeling study. *Antivir Res* 95:118–127
- Balzarini J, Orzeszko-Krzesinska B, Maurin JK, Orzeszko A (2009) Synthesis and anti-HIV studies of 2- and 3-adamantyl-substituted thiazolidin-4-ones. *Eur J Med Chem* 44:303–311
- Brittelli David R (1981) Phosphite-mediated in situ carboxyvinylolation: a new general acrylic acid synthesis. *J Org Chem* 46:2514–2520
- Chen DF, Zhang SX, Xie L et al (1997) Anti-AIDS agents—XXVI. Structure-activity correlations of gomisin-G-related anti-HIV lignans from *Kadsura interior* and of related synthetic analogues. *Bioorg Med Chem* 5:1715–1723
- Chen H, Ma YB, Huang XY, Geng CA, Zhao Y, Wang LJ, Guo RH, Liang WJ, Zhang XM, Chen JJ (2014) Synthesis, structure-activity relationships and biological evaluation of dehydroandrographolide and andrographolide derivatives as novel anti-hepatitis B virus agents. *Bioorg Med Chem Lett* 24:2353–2359
- Du NN, Li X, Wang YP, Liu F, Liu YX, Li CX, Peng ZG, Gao LM, Jiang JD, Song DQ (2011) Synthesis, structure-activity relationship and biological evaluation of novel N-substituted matrix acid derivatives as host heat-stress cognate 70 (Hsc70) down-regulators. *Bioorg Med Chem Lett* 21:4732–4735
- Ferrari M, Fornasiero MC, Isetta AM (1990) MTT colorimetric assay for testing macrophage cytotoxic activity in vitro. *J Immunol Methods* 131:165–172
- Gao LM, Han YX, Wang YP, Li YH, Shan YQ, Li X, Peng ZG, Bi CW, Zhang T, Du NN, Jiang JD, Song DQ (2011) Design and synthesis of oxymatine analogues overcoming drug resistance in hepatitis B virus through targeting host heat stress cognate 70. *J Med Chem* 54:869–876
- Han YQ, Huang ZM, Yang XB, Liu HZ, Wu GX (2008) In vivo and in vitro anti-hepatitis B virus activity of total phenolics from *Oenanthe javanica*. *J Ethnopharmacol* 18:148–153
- Karakurt A, Mehmet AA, Burcu S, Çalis Ü, Dalkara S (2012) Synthesis of some novel 1-(2-naphthyl)-2-(imidazol-1-yl)ethanone oxime ester derivatives and evaluation of their anticonvulsant activity. *Eur J Med Chem* 57:275–282
- Kim SN, Lee JY, Kim HJ, Shin CG, Parka H, Lee YS (2000) Synthesis and HIV-1 integrase inhibitory activities of caffeoylglucosides. *Bioorg Med Chem Lett* 10:1879–1882
- Lavanchy D (2004) Hepatitis B virus epidemiology, disease burden, treatment, and current and emerging prevention and control measures. *J Viral Hepat* 11:97–107
- Liu JX, Kenneth Y, Chen ECR (2011) Structural insights into the binding of hepatitis B virus core peptide to HLA-A2 alleles: towards designing better vaccines. *Eur J Immunol* 41:2097–2106
- Liu S, Wei WX, Shi KC, Cao X, Zhou M, Liu ZP (2014a) In vitro and in vivo anti-hepatitis B virus activities of the lignan niranthin isolated from *Phyllanthus niruri* L. *J Ethnopharmacol* 155:1061–1067
- Liu S, Wei WX, Li YB, Lin X, Shi KC, Cao X, Zhou M (2014b) In vitro and in vivo anti-hepatitis B virus activities of the lignan nirtetralin B isolated from *Phyllanthus niruri* L. *J Ethnopharmacol* 157:62–68
- Liu S, Wei WX, Li YB, Liu X, Cao XJ, Lei KC, Zhou M (2015) Design, synthesis, biological evaluation and molecular docking studies of phenylpropanoid derivatives as potent anti-hepatitis B virus agents. *Eur J Med Chem* 95:473–482
- Manat M, Patil B (2007) Evaluation of antiinflammatory activity of methanol extract of *Phyllanthus amarus* in experimental animal models. *Indian J Pharm Sci* 69:33
- Ovenden SP, Yu J, San WS et al (2004) Globoidnan A: a lignan from *Eucalyptus globoidea* inhibits HIV integrase. *Phytochemistry* 65:3255–3259
- Panda P, Appalashetti M, Natarajan M, Mary CP, Venkatraman SS, Judeh ZMA (2012a) Synthesis and antiproliferative activity of helonioside A,3',4',6'-tri-O-feruloylsucrose, lapathoside C and their analogs. *Eur J Med Chem* 58:418–430
- Panda P, Appalashetti M, Natarajan M, Chan-Park MB, Venkatraman SS, Judeh ZMA (2012b) Synthesis and antitumor activity of lapathoside D and its analogs. *Eur J Med Chem* 53:1–12

- Parvathaneni M, Battu GR, Gray AI et al (2014) Investigation of anticancer potential of hypophyllanthin and phyllanthin against breast cancer by in vitro and in vivo methods. *Asian Pac J Trop Dis* 4:S71–S76
- Peterson JR, Russell ME, Surjasmita IB (1988) Synthesis and experimental ionization energies of certain (E)-3-arylpropenoic acids and their methyl esters. *J Chem Eng Data* 33:534–537
- Quan VV, Trenerry C, Rochfort S, Wadeson J, Leyton C, Hughes AB (2013) Synthesis and anti-inflammatory activity of aromatic glucosinolates. *Bioorgan Med Chem* 21:5945–5954
- Saleem M, Kim HJ, Ali MS et al (2005) An update on bioactive plant lignans. *Nat Prod Rep* 22:696–716
- Salum ML, Robles CJ, Erra-Balsells R (2010) Photoisomerization of ionic liquid ammonium cinnamates: one-pot synthesis-isolation of Z-cinnamic acids. *Org Lett* 12:4808–4811
- Salway AH (1909) Synthesis of substances allied to cotarnine. *J Chem Soc Trans* 95:1204–1220
- Santos FD, Abreu P, Castro HC, Paixao ICPP, Cirne-Santos CC, Giongo V, Barbosa JE, Simonetti BR, Garrido V, Bou-Habib DC, Silva DD, Batalha PN, Temerozo JR, Souza TM, Nogueira CM, Cunha AC, Rodrigues CR, Ferreira VF, Souza MCBV (2009) Synthesis, antiviral activity and molecular modeling of oxoquinoline derivatives. *Bioorgan Med Chem* 17:5476–5481
- Terent'ev AO, Krylov IB, Ogibin YN, Nikishin GI (2006) Chlorination of oximes with aqueous H₂O₂/HCl system: facile synthesis of gem-chloronitroso- and gem-chloronitroalkanes, gem-chloronitroso- and gem-chloronitrocycloalkanes. *Synthesis* 22:3819–3824
- Viegas-Junior C, Danuello A, Bolzani VS, Barreir EJ, Fraga CAM (2007) Molecular hybridization: a useful tool in the design of new drug prototypes. *Curr Med Chem* 14:1829–1852
- Wang LJ, Geng CA, Ma YB, Huang XY, Luo J, Chen H, Guo RH, Zhang XM, Chen JJ (2012) Synthesis, structure–activity relationships and biological evaluation of caudatin derivatives as novel anti-hepatitis B virus agents. *Bioorg Med Chem Lett* 20:2877–2888
- Wei WX, Li XR, Wang KW, Zheng ZW, Zhou M (2012) Lignans with anti-hepatitis B virus activities from *phyllanthus niruri* L. *Phytother Res* 26:964–968
- Wu ZR, Zheng LF, Li Y, Su F, Yue XX, Tang W, Ma XY, Nie JY, Li HY (2012) Synthesis and structure–activity relationships and effects of phenylpropanoid amides of octopamine and dopamine on tyrosinase inhibition and antioxidation. *Food Chem* 134:1128–1131
- Yamashita K, Nohara Y, Katayama K et al (1992) Sesame seed lignans and gamma-tocopherol act synergistically to produce vitamin E activity in rats. *J Nutr* 122:2440–2446
- Zou HB, Wu H, Zhang XN, Zhao Y, Joachim S, Lou YJ, Yu YP (2010) Synthesis, biological evaluation, and structure-activity relationship study of novel cytotoxic aza-cafeic acid derivatives. *Bioorgan Med Chem* 18:6351–6359